ELSEVIER

Nuclear Physics A682 (2001) 439c–448c

NUCLEAR PHYSICS A

www.elsevier.nl/locate/npe

Coupling between thermal and rotational motion in nuclei

T. Døssing[a], B. Herskind[a], M. Matsuo[b], S. Leoni[c], A. Bracco[c], E. Vigezzi[c], and R.A. Broglia[a,c]

[a]Niels Bohr Institute, University of Copenhagen, DK2100 Copenhagen Ø, Denmark

[b]Graduate School of Science and Technology, Niigata University, Niigata 950-2181, Japan

[c]INFN sez Milano, and Department of Physics, University of Milano, Milan 20133, Italy

Two aspects of rotational motion of thermally excited nuclei are discussed. First, the schematic cases of ordered or chaotic motion of intrinsic and rotational motion are presented: discrete rotational bands, ergodic bands, damping of the rotational motion. Secondly, the strength functions of mixing of basis bands and of E2-transitions over one or two decay steps are discussed. The two-step E2-strength displays both a narrow and wide component, yielding different types of information about the basis bands and their interaction. Indications of the presence of a narrow component is found in energy correlations of consecutive transitions on displaced rotational bands of a three dimensional spectrum for the nucleus ^{168}Yb.

1. INTRODUCTION

A heavy-ion fusion reaction produces a compound nucleus which carries both temperature and rotation. The compound nucleus decays via a cascade of particles and γ-rays, which cools down the nucleus and slows its rotation, eventually reaching the ground state.

The first decay steps, predominantly emission of nucleons or α-particles, but also high-energy γ-rays, provide strong cooling without changing the rotational frequency very much. The temperature present at these stages of the decay cascade implies statistical averaging over a large number of nuclear states, and the study of decay products can only yield overall properties, such as the average rotational frequency, the distribution of shapes and orientations etc. Especially, investigations of the giant dipole resonance at temperatures in the interval $T \sim 1-3$ MeV have been fruitful, yielding information about doorway coupling mechanisms and shape fluctuations in the presence of temperature, as well as about the time-scale for exciting the dipole mode [1,2].

In the following decay steps, a long cascade of γ-rays, the bulk part of the rotation is slowed down, while gradually also cooling the nucleus towards its ground state. Typically, the cascade takes place at a temperature around $T \sim 0.25 - 0.50$ MeV [3,4]. Resolving individual γ-lines and building level schemes for this temperature range is not possible with present day techniques.

Actually, the first experiments on rapidly rotating nuclei, carried out by Stephens,

0375-9474/01/$ – see front matter
PII S0375-9474(00)00671-0

Diamond and collaborators, dealt with averages over many states. Fine examples are given by the correlation between γ-ray energy and multiplicity [5], and angular correlations of γ-rays [6]. Such experiments showed that collective rotation with the emission of stretched electric quadrupole transitions occurs up to the highest angular momenta which the nucleus can accommodate. On this basis, it was expected that the E2 γ-cascades would proceed down through rotational bands. However, with the study of energy-energy correlation spectra by Herskind and collaborators [7,8] it became clear that the highly correlated γ-ray sequences characteristic of rotational bands are more the exception than the rule for the cascades. Leander was the first to suggest that the presence of temperature causes the rotational bands to become mixed, implying a spreading of the E2 decay over many states, destroying the strong energy-correlations [9]. Subsequent experiments have confirmed this picture, which later has been named "damping of the rotational motion" [10].

Chapter 2 of the present paper gives a discussion of rotation of warm nuclear states, with reference to the general notions of ordered and chaotic motion. Recent theoretical developments have shed light on the strength functions for spreading of basis bands and its relation to two-dimensional γ-ray spectra, as will be discussed in section 3. This leads up to section 4, which shows some current efforts at extracting such strength functions. Section 5 contains a conclusion.

2. ROTATING WARM STATES

Figure 1 shows in a schematic way the different modes of rotation of a well deformed nucleus. With the present-day techniques, studies of discrete γ-rays of deformed nuclei address discrete rotational bands. To assign quantum numbers for intrinsic states to such bands only has meaning if the intrinsic structure is well defined, i.e. is "ordered" in the present schematic terminology. Success criteria for such assignments concern selection rules for transitions across bands, as well as the development with rotational frequency of the moment of inertia, which shows the response of the intrinsic structure to rotation.

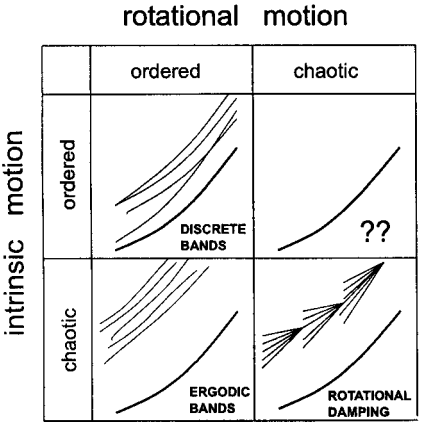

Figure 1. Schematic drawing of energy versus angular momentum of the states emitting rotational γ-rays in the extreme modes of rotation of a deformed nucleus, determined by the order-chaos properties of intrinsic states and of the rotational motion. On each panel, the yrast discrete band is denoted by a thick line.

It is well known that the quantum states at low angular momenta become "chaotic" around temperature $T \sim 0.7$ MeV (the numbers here refer to rare-earth nuclei), that is chaotic in the simplest sense of level distance distributions and transition strength distributions. Chaotic intrinsic states might still be combined with ordered rotational motion, forming ergodic rotational bands, as discussed first by Bohr and Mottelson [11], and later more quantitatively by Åberg [12]. In terms of wave-functions, this scenario implies that the admixture of the wavefunction only changes slowly from one angular momentum to the next, when expressed in a basis of rotational bands, which diagonalize the E2 transition operator. Such a basis is not unique, which leaves some room for doubts about calculations of mixed rotational bands. One can understand that the existence of ergodic bands must rely on having a big nucleus of a large deformation. In that case, most of the orbitals will be strongly coupled to the deformed shape, and the rotational frequency changes little from one angular momentum to the next. Good candidates for ergodic bands may be excited superdeformed bands in the mass A $\sim$ 190 region [16], or hyperdeformed bands [13].

For well deformed rare earth and lighter nuclei, a good part of the orbitals are appreciably affected by rotation. If the basis bands are generated from such orbitals, the band mixing will be different at neighbouring angular momenta differing by two units, and the E2 matrix elements will be spread out over many states. This is the scenario of damping of the rotational motion, described first by Leander [9]. Later, quantitative estimates of strength functions etc. have been carried out with a schematic cranking model by Lauritzen *et al.* [10], and more consistently with the cranking model by Åberg [14,12] and by Matsuo *et al.* [15]. Despite the spreading out of the E2 strength to many final states, the strength function is predicted to have a rather narrow width, the rotational damping width, of about $\Gamma_{rot} \approx 250$ keV, with substantial dependence on mass number and deformation [16,17].

The last possible schematic mode, ordered intrinsic motion and chaotic rotational motion, is probably not realistic for nuclei.

In figure 1, the coldest bands are drawn as discrete bands, and the other two scenarios are drawn for an interval of excited states. For rare earth nuclei, the cranking model predicts a transition from discrete to damped rotation at an excitation energy above yrast of about 700 keV. This prediction has been confirmed by an analysis of fluctuations of two-dimensional spectra [18].

Presently, level schemes of rotating nuclei can be rather complete up to around 500 keV of heat energy (that is the energy above yrast), with about 20 resolved rotational bands of the four parity-signature combinations. With the development of more powerful γ-detection systems in the near future, it should be possible to construct level schemes displaying branching on several final states, in the region of the onset of damping of the rotational motion.

Until now, two applications of resolved transitions have addressed the average properties of bands, relevant to the present discussion, and they both display a tendency away from the fully ordered situation. The analysis of level spacings carried out by Garrett and coworkers have exhibited "the most Poisson-like distribution in nuclear physics" [19]. This is in full accordance with the meaningful structure assignments to most of the rotational bands in the region of resolved spectra. However, the data also show a tendency to avoid

the smallest spacings, indicating interactions between the bands. Interactions among crossing bands lead to a local branching of the E2-transitions on two final states. This branching can be viewed as a precursor to damping of the rotational motion. A careful analysis of such crossings by Bark, Hagemann *et al.,* [20] allowed for extracting the size of the matrix elements at several crossings. The average r.m.s. of the extracted interaction $\sqrt{\langle|V_{2-body}|^2\rangle}$ is about $10-15$ keV, in reasonable agreement with calculations based on the surface-δ interaction [15].

In the following sections we address the transitions from ordered to chaotic motion, that is the intermediate situation between the upper left panel and lower right panel, by investigating rotational transition strength functions of two and three dimensional spectra. It turns out that remnants of the basis bands, which are related to the discrete bands in the ordered situation, will be present well into the damped situation.

3. STRENGTH FUNCTIONS FOR $\Delta I = 0, -2, -4$

Two-dimensional γ-spectra probe the energy correlations between two decay steps of the cascade. Most interesting are consecutive rotational transitions, from which one may extract information about the nature of the basis rotational bands and of the interaction which mixes them and causes damping.

Locally, at one value of the angular momentum I, the mixing of each basis band state $|\mu\rangle$ is described by the strength function

$$S_\mu(E) = \sum_\alpha |\langle\alpha|\mu\rangle|^2 \delta(E - E_\alpha)$$

where $\langle\alpha|\mu\rangle$ is the amplitude of $|\mu\rangle$ in the energy eigenstate $|\alpha\rangle$, at energy E_α. The spreading in energy of the basis band state $|\mu\rangle$ is given by the autocorrelation function

$$C_\mu(e) = \int S_\mu(E+e) S_\mu(E) dE$$

which expresses the probability of pairwise strengths in S_μ being located at a distance e in energy. The autocorrelation function $C_\mu(e)$ has the physical interpretation as the Fourier transformation of the survival probability $P_\mu(t) = |\langle\mu|e^{-iHt}|\mu\rangle|^2$ of staying in the basis band after a time t.

Here, it is very important to use the autocorrelation function and not the strength functions itself, the reason being that the average energy $\bar{E}_\mu$ of the strength function may be influenced by small components, shifted far away from the centroid. This produces an extra width when taking averages of the strength function. Such far-away components arise from the large matrix elements of the residual interaction, for example the surface-δ interaction, as discussed and illustrated in reference [21].

The autocorrelation function, when averaged over intervals of energy of the basis bands, expresses a $\Delta I = 0$ strength function, that is the formation of mixed bands locally at one given angular momentum. An example is shown on figure 2, upper left panel, calculated with a standard shell model for warm rotating nuclei [15] with cranked mean field bands interacting via the surface-δ interaction. The result is shown for states around $U \sim 1.5$ MeV of heat energy, where the level spacing of each parity-signature is approximately $\rho^{-1} \sim 5$ keV.

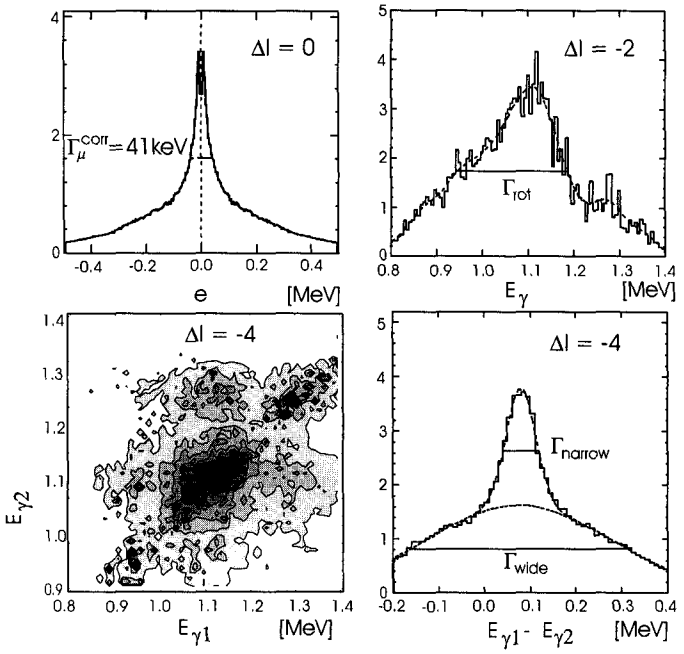

Figure 2. $\Delta I = 0$, -2, and -4 average strength functions, averaged over level number 51 to 100 of each parity-signature, located in an interval of heat energy between 1.5 MeV and 1.8 MeV. Upper left panel displays the local mixing of basis band states, the $\Delta I = 0$ distribution, for which the autocorrelation function is applied, and the averaging over angular momentum is from $30 - 50$. The upper right panel displays the $\Delta I = -2$ distribution of γ-ray energies, and the bottom panels show the $\Delta I = -4$ distribution, as contour plots and projected, both averaged over angular momenta $42 - 43$.

At this heat energy, the E2 decay out of each energy-eigenstate $|\alpha\rangle$ typically branches out to 5 states at angular momentum $I - 2$. The average strength function for this decay is shown on figure 2, upper right panel. This $\Delta I = -2$ distribution and its width, the rotational damping width, has the original interpretation described by Lauritzen *et al.*, [10]: At the heat energy in question for figure 2, and for the decay flow in rare earth nuclei generally, the E2 strength distribution reflects the distribution of rotational frequencies present in the basis bands before their mixing. (for higher heat energies, the distribution may become more narrow, interpreted as "motional narrowing" [10,23]).

The two lower panels of figure 2 shows the two-dimensional strength function, on a contour plot on the left hand side, and projected on the upper-left - lower-right diagonal on the right hand side, that is a projection on an axis $E_1 - E_2$ of the two transition energies. The projected $\Delta I = -4$ strength function clearly displays two components, and it turns out that the width of the narrow component is roughly proportional to the spreading width of the basis band states, about twice as wide: $\Gamma_{narrow} \sim 2\Gamma_\mu^{corr}$, the subscript

"corr" denoting the use of the autocorrelation function in extracting the spreading width.

For a given interval in heat energy, the narrow component contains the most intense transitions [22,15], and the connection between the widths Γ_{narrow} and Γ_{μ}^{corr} can qualitatively be understood as arising from the strength fluctuations in the mixing coefficients $|\langle\alpha|\mu\rangle|^2$. For low heat energies, such fluctuations are generated by the fluctuations in the size of matrix elements and level spacings of pairwise interacting levels, while for higher heat energies they will approach Porter-Thomas fluctuations, characteristic of chaotic motion. For each basis state at consecutive angular momenta $|\mu(I)\rangle$, $|\mu(I-2)\rangle$ and $|\mu(I-4)\rangle$, these fluctuations in mixing coefficients ensure the existence of energy eigenstates $|\alpha(I)\rangle$, $|\alpha'(I-2)\rangle$ and $|\alpha''(I-4)\rangle$, carrying strong components of $|\mu\rangle$. The rather intense B(E2) transition moment $\alpha \rightarrow \alpha' \rightarrow \alpha''$ give an intense contribution to the $\Delta I = -4$ strength function. Summing over the energy eigenstates at angular momenta I and $I-4$, the contribution to the narrow component from each basis band state has the form of a correlation function between the strength functions $S_{\mu}(E)$ at I and $I-4$. Finally, summing over energy eigenstates at $I-2$ and over basis band states, one finds the above mentioned result for the widths, $\Gamma_{narrow} \sim 2\Gamma_{\mu}^{corr}$. Furthermore, one finds that the intensity of the narrow component should roughly be inversely proportional to the spreading number, which is the effective number of basis band states mixed into each energy eigenstate. This overall picture is confirmed by detailed calculations with the cranked shell model and the surface-δ interaction [21]. For the cranked shell model, the basis bands are the excited rotating mean field states, and the spreading width Γ_{μ}^{corr} in energy remains rather small for the interesting energy region $U \sim 1.5$ MeV, $\Gamma_{\mu}^{corr} \approx 40$ keV.

These considerations concerning the two-component structure of the two-dimensional $\Delta I = -4$ transition strength function also apply if the basis bands would be of another nature. Transition strength fluctuations and fluctuations of admixture coefficients are expected to occur generally. The width of the narrow $\Delta I = -4$ component of two-dimensional γ-spectra would still be twice the spreading width of the basis band state, while the width of the wide component would still be about $\sqrt{2}$ times the dispersion of the rotational frequency among basis band states.

4. RIDGES IN THREE DIMENSIONAL SPECTRA

Strength functions such as the ones shown in figure 2 are for the moment outside the reach of experiments. From the long cascades, it is not possible to separate consecutive transitions, and especially it is not possible to gate on a specific interval in heat energy.

In searching for the narrow component, we are looking at three-dimensional spectra, where the rotational energy correlations are emphasised by slicing out *rotational planes* of the three dimensional cube. The rotational plane is given by the equation:

$$E_1 + E_2 - 2E_3 = 0 \qquad \text{(rotational plane)}$$

as illustrated in a standard coordinate system in figure 3.

A perfect rotational band of a rigid rotor, or a band which has a constant moment of inertia within an interval of angular momentum, will place its transitions on the rotational plane, in the sequences E_1, E_3, E_2 or E_2, E_3, E_1. Several rotational bands with different frequency displacements and variations in the moment of inertia will form a ridge.

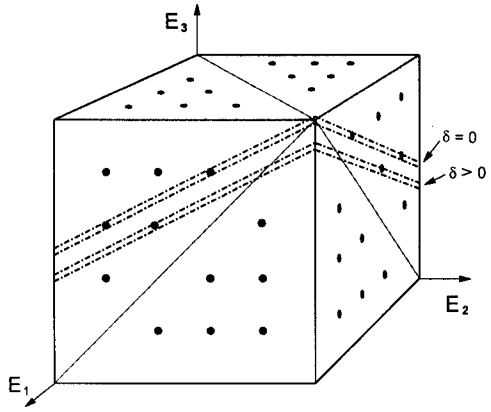

Figure 3. Illustration of coincidences of a three dimensional spectrum. The location of coincidences along a perfect rotational band (dots), and the "side-valleys" (dashed lines) are shown on the faces of the cube. The rotational plane and a displaced plane (dot-dashed lines) are illustrated with a certain width, corresponding to the experimental situation, where a slice is cut out of the cube, and then projected down onto the E_1 versus E_2 plane.

Figure 4 shows the rotational plane of the Compton and peak subtracted three dimensional spectrum, extracted from an experiment on the γ-detector array EUROGAM. The plane is produced by a rather thin slice of the cube, only one channel wide, that is 4 keV in the vertical direction on figure 3. A pronounced ridge is seen, and the value of $E_1 - E_2$ at the ridge is $8/\mathcal{I}^{(2)}_{band}$, where $\mathcal{I}^{(2)}_{band}$ is the second moment of inertia of rotational bands. The second moment of inertia is seen to decrease with rotational frequency up to about 450 keV, (transition energy about 900 keV), where it starts to increase again. This behaviour is also seen for the resolved bands for the nuclei ^{167,168}Yb, whose coincidences are removed on the figure. Thus, the figure shows that the excited bands behave in much the same way with respect to the moment of inertia as the resolved bands. Other features of figure 4 are not seen in resolved bands, as for example the "bridge" across the valley around transition energy 1020 keV, which is a kind of "backbend" of many bands, maybe related to the multiband crossings described in ref. [8].

Irregularities in the energies of the bands will cause the coincidences in three dimensional spectra to be kicked a little out of the rotational plane, to fall on a displaced rotational plane:

$$E_1 + E_2 - 2E_3 = \delta \qquad \text{(displaced rotational plane)}$$

where δ may be denoted the displacement energy.

To examine the ridges in more detail, the rotational planes are projected onto a $E_1 - E_2$ axis, within intervals of width 60 keV $\approx 4/\mathcal{I}^{(2)}$ in $(E_1 + E_2)/2$. Figure 5 displays such projections of displaced rotational planes, together with the equivalent spectra calculated by simulations of the γ-cascades. The simulations are of the type described in reference [24]. The figure shows a strong similarity between data and simulations. (Due to the lack of explicit treatment of the pairing interaction in the cranked mean field states underlying the simulations, they are terminated at a lower angular momentum of 20, cutting off rotational transitions beyond $|E_1 - E_2| \geq 300$ keV in the figure.)

Roughly one third of the ridge should be due to the narrow component discussed in the previous section. The fragmented decay generating the narrow component, as opposed to decay along a discrete band, should imply larger values of the displacement energy δ.

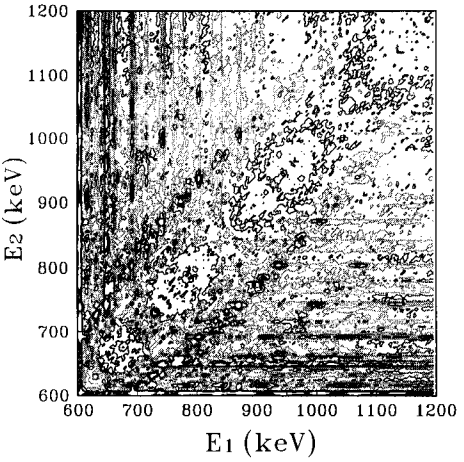

Figure 4. Contour plot of the rotational plane for the EUROGAM data after Compton subtraction and subtraction of peaks corresponding to known discrete lines. Contours in the valley at $E_1 = E_2$ surround minima, and contours at the ridges at $E_1 = E_2 \pm 120$ keV surround maxima.

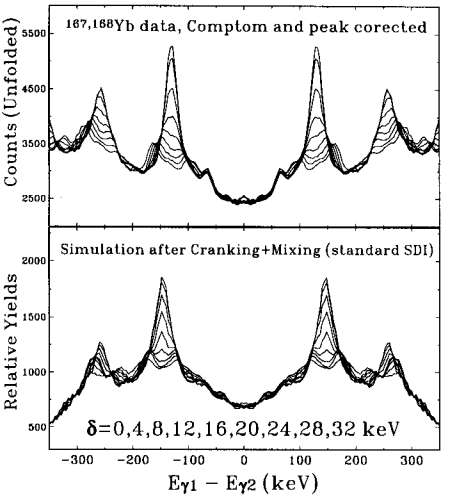

Figure 5. Projections on the coordinate $E_1 - E_2$ of the rotational plane from figure 4 and of displaced rotational planes, performed for the interval of transition energy of $(E_1 + E_2)/2 = 830 - 890$ keV. The most intense ridge corresponds to the unshifted plane $\delta = 0$, while the height of the ridge decreases with increasing displacement energy $\delta = 4, 8, 12, \cdots$ keV.

To see whether such expectations materialise in the data, we have investigated the ridge fluctuations for the various slices. The resulting number of paths are shown in figure 6, for four different values of the rotational energy $(E_1 + E_2)/2$. Except for the lowest energy, 740 keV, the number of paths increases with increasing δ, up to around 20 keV, beyond which the ridge is harder to trace (cfr. fig. 5). For example, for $\delta = 20$ keV, the intensity of the ridge is about 1/4 of that at $\delta = 0$, and the number of paths is about 3/2 as many, such that the average intensity of the transitions in the ridge at $\delta = 20$ keV is down by a factor of about $\frac{1}{6}$ relative to $\delta = 0$.

This result is compared in figure 7 to the behaviour of resolved bands, for which the displacement δ for each set of three consecutive transitions can be calculated directly. The number of resolved bands is seen to undershoot the number of bands in the ridge by a substantial amount. This is partly due to the fact that the experiment samples three final nuclei, ^{167,168,169}Yb. More pronounced in the figure is the relative dependence on displacement. With increasing δ, the number of resolved bands decreases dramatically for ^{168}Yb, and somewhat more slowly for ^{163}Er, both displaying a completely different behaviour than the unresolved transitions in the ridge. We attribute this behaviour to the presence of the narrow component, and the results of figures 6 and 7 are in accordance

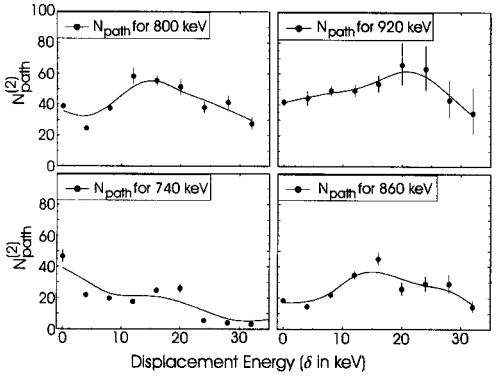

Figure 6. Number of decay paths in the ridge of figure 5 shown as function of the displacement energy, calculated for different values of the centroid of 60 keV wide intervals in $(E_1 + E_2)/2$.

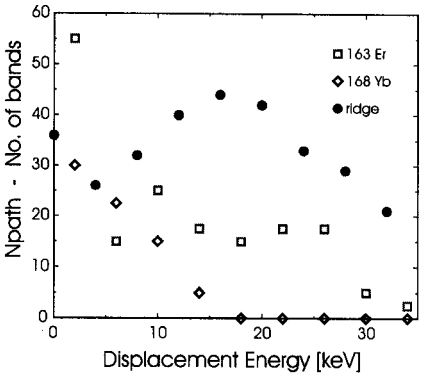

Figure 7. Average of the experimental number of decay paths in the displaced ridges from figure 6 compared to the equivalent distribution of displacement energies of resolved bands for two nuclei. The values for the resolved bands are multiplied by a factor of 10.

with the following picture: The most intense bands, closest to the yrast line, are the most regular, yielding coincidences with small displacement. With increasing excitation energy above yrast, the bands start to interact, and the E2 transitions eventually fragment, yielding more and weaker transitions spread out over a larger interval of displacement energy δ.

The FWHM of the ridge in the displacement is only about 32 keV, and we are not able yet to relate it to the spreading width of basis band states. This is partly caused by one disadvantage of this analysis, namely that is does not furnish a clean separation between discrete-band transitions and transitions from the damped regime. We have searched several places in the three-dimensional cube for regions where the narrow component of the damped decay might stand out, avoiding contamination from coincidences with discrete bands, sofar without success.

5. CONCLUSION

We have described the characteristic modes of rotation in excited deformed nuclei, with reference to order-chaos properties of rotational states and transitions: discrete bands, ergodic bands, and damping of the rotational motion.

Theoretical two-dimensional E2 strength distributions calculated with a basis of independent particle cranking model bands, interacting via a two-body surface-δ interaction display a two-component structure. Most interesting here are states in the interval of heat energy where the gradual transition from discrete bands to damped rotation takes place. A narrow component of the two-dimensional strength is related to the local mixing of

basis band states, and a wide component is related to the different rotational frequencies present in the basis bands.

A search for the narrow component is performed in three-dimensional spectra, projecting out the rotational plane and shifted rotational planes. This emphasises rotational energy correlations, along perfect rotational bands at the undisplaced rotational plane, at displacement energy zero, and bands with increasing irregularity with increasing displacement. A fluctuation analysis of the ridges on these planes show first an increase in the number of decay paths (that is the effective number of coincidences) as function of displacement energy, then a decrease. The equivalent number of coincidences along resolved bands has a rather narrow maximum around displacement zero, that is the resolved bands display much more regular rotational sequences than the ridge in general. This is taken as an indication that the wider part of the ridge is actually due to the narrow component of transitions from states in the heat energy interval of onset of damping of the rotational motion. A more quantitative understanding of the width of the ridge, as well as of the behaviour of the number of paths with displacement energy, has not been achieved yet.

REFERENCES

1. Y. Alhassid, Nucl. Phys A649 (1999) 107c, and refs. therein.
2. F. Camera *et al.*, Nucl. Phys A649 (1999) 115c, and refs. therein.
3. J. Garrett, G. B. Hagemann and B. Herskind, Ann. Rev. Nucl. Part. Sci. 36 (1986) 419.
4. T. Døssing and E. Vigezzi, Nucl. Phys A587 (1995) 13.
5. M. A. Deleplanque *et al.*, Phys. Rev. Lett 40 (1978) 629.
6. M. A. Deleplanque *et al.*, Phys. Rev. Lett 41 (1978) 1105.
7. O. Andersen *et al.*, Phys. Rev. Lett. 43 (1979) 687.
8. B. Herskind, Journal de Physique c-10 (1980) 106.
9. G. A. Leander, Phys. Rev. C25 (1982) 2780.
10. B. Lauritzen, T. Døssing, and R. A. Broglia, Nucl. Phys. A457 (1986) 61.
11. Aa. Bohr and B. Mottelson, Physics Scripta 24 (1981) 71.
12. S. Åberg, Prog. Nucl. and Part. Phys. 28 (1992) 11.
13. S. Åberg, Nucl. Phys. A557 (1992) 17c.
14. S. Åberg, Phys. Rev. Lett. 26 (1990) 3119.
15. M. Matsuo *et al.*, Nucl. Phys. A617 (1997) 1.
16. K. Yoshida and M. Matsuo, Nucl. Phys. A636 (1998) 169.
17. M. Matsuo *et al.*, Nucl. Phys. A649 (1999) 379c.
18. T. Døssing *et al.*, Phys. Rep. 268 (1996) 1.
19. J. D. Garrett *et al.*, Phys Lett B392 (1997) 24.
20. G. B. Hagemann *et al.*, Nucl. Phys A618 (1997) 199,
    J. M. Espino *et al.*, Nucl. Phys. A640 (1998) 163.
21. M. Matsuo *et al.*, Phys. Lett. 465 (1999) 1.
22. S. Leoni *et al.*, Nucl. Phys A587 (1995) 513.
23. R. A. Broglia *et al.*, Phys. Rev. Lett. 58 (1987) 326.
24. A. Bracco *et al.*, Phys. Rev. Lett. 76 (1996) 4484.